

# Development of Local Scantling Formulae for Plate Members

Tetsuo OKADA\*

## 1. INTRODUCTION

Plate members are one of the most essential elements in a ship structure consisting of stiffened panels. Plates are subjected to bending due to lateral pressure from water pressure, cargoes, etc. In-plane stresses also act on plates used in stiffeners, primary supporting members and the members of hull girders, and the magnitude of that stress is particularly remarkable for bending and shearing of hull girders. In the design of plate members, it is necessary to evaluate various damage modes, including bending under lateral pressure and buckling and yielding under in-plane loading. In particular, however, local strength equations for bending due to lateral pressure are extremely important for determining the initial plate thickness in the earliest stage of basic design <sup>1)</sup>.

Theories of the strength of plate members for out-of-plane (lateral) loading have been established based on plastic design, rigid-plastic analysis and other approaches <sup>2)3)</sup>, and simplified plate local scantling formulae based on those theories are provided in ship classification rules. The former Rules of Nippon Kaiji Kyokai (ClassNK) were based on safety factors which were given empirically for 3-point plastic hinge formation of a plate strip between stiffeners <sup>4)</sup>, and considered the reduction of fully plastic moment under the simultaneous action of lateral loading and in-plane stress by using the von Mises yield criterion for transversely framed structures and Tresca's yield criterion for longitudinally framed structures <sup>5)</sup>. In the Common Structural Rules (CSR) <sup>6)</sup>, correction is performed by using a permissible bending stress coefficient set by an elasto-plastic FEM analysis, in which in-plane stress is also made to act simultaneously based on the formation of a 3-point plastic hinge. The safety of these scantling formulae has been confirmed from the actual track records over many years. However, for application to more complex combinations of structural behaviors and loads, reviewing those formulae to develop scantling formulae which have a theoretical backing and a clearer correspondence with damage was an issue. This paper presents an outline of the following items, which were carried out as part of that review <sup>7)8)9)</sup>.

- As the basic theory that serves as the foundation for the scantling formulae, the reduction of the fully plastic moment by superimposition of bending and in-plane stress was expressed by the von Mises yield criterion for both the transversely framed and longitudinally framed structural systems. Furthermore, theoretical study by obtaining the 2-point and 3-point plastic hinge formation loads, also considering the additional lateral load (term proportional to the curvature of plate bending) generated accompanying in-plane stress, was adopted as a basis.
- The influence of in-plane stress on the lateral pressure that causes a certain designated residual deflection in analysis by elasto-plastic FEM was investigated in detail and compared with the results by the theoretical equations, and a rational in-plane stress influence factor was proposed for plate members of laterally and longitudinally framed structures.
- In the conventional ship classification society rules, the aspect ratio (ratio of the lengths of the longer and shorter edges) was considered independently from the effect of in-plane stress. However, in cases where in-plane stress influence factors are differentiated for a transversely framed structure and a longitudinally framed structure, discontinuity arises when the aspect ratio is larger or smaller than 1, and it is not possible to reflect the actual phenomena. Therefore, an equation for interpolation of the in-plane stress factor between lateral and longitudinal framing systems was proposed for small aspect ratios.

---

\* Faculty of Engineering, Yokohama National University

## 2. THEORETICAL EQUATION FOR PLATE BENDING STRENGTH CONSIDERING IN-PLANE STRESS

### 2.1 Influence of In-Plane Stress on Fully Plastic Moment

#### 2.1.1 Transversely Framed Structures

Chapter 2 and Chapter 3 consider the case of plates with an extremely large aspect ratio, and therefore treat bending of plates as bending of a plate strip. First, as shown in Fig. 1, the case in which a member receives in-plane stress in the direction perpendicular to the longer edge of the plate as a transversely framed structure is considered. The object of study is the bending behavior of the portion of the plate strip indicated by the hatching, whose span as a beam is assumed to be the spacing between stiffeners.

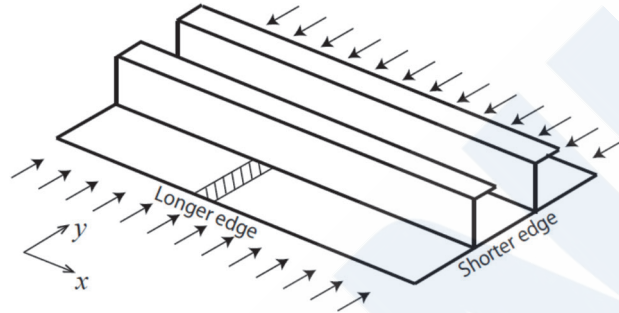


Fig. 1 Model of plate bending (transversely framed structure)

In this case, because bending stress and in-plane stress act in the same direction, the fully plastic moment  $M_p$  decreases according to Eq. (1) in comparison with the case without in-plane stress. The former ClassNK Rules considered the influence of in-plane stress based on this equation <sup>5)</sup>.

$$M_p = \frac{\alpha \sigma_Y t^2}{4} \left\{ 1 - \left( \frac{\sigma_y}{\sigma_Y} \right)^2 \right\} \quad (1)$$

$t$  : plate thickness

$\sigma_y$  : in-plane stress acting in  $y$  direction

$\sigma_Y$  : specified yield stress of material

$\alpha$  : Because the direction orthogonal to the stress perpendicular to the  $y$  direction is constrained,  $\alpha$  is considered as a coefficient which expresses the fact that stress perpendicular to the  $y$  direction exceeding the specified yield stress is generated when the material yields by the von Mises yield criterion, and is given by Eq. (2):

$$\alpha = \sqrt{\frac{1}{1 - \nu_p + \nu_p^2}} = \frac{2\sqrt{3}}{3} = 1.15 \quad (2)$$

$\nu_p$  : Poisson's ratio in plastic state;  $\nu_p = 0.5$

From Eq. (1), the effect of the action of in-plane stress on the fully plastic moment can be obtained from the following equation as the ratio of  $M_p$  and the fully plastic moment  $M_{p0}$  when in-plane stress does not act.

$$\frac{M_p}{M_{p0}} = 1 - \left( \frac{\sigma_y}{\sigma_Y} \right)^2 \quad (3)$$

Because the required plate thickness  $t$  is inversely proportional to the square root of this, it is obtained as a ratio to  $t_0$  when an axial load does not act as follows:

$$\frac{t}{t_0} = \frac{1}{\sqrt{1 - \left(\frac{\sigma_y}{\sigma_Y}\right)^2}} \quad (4)$$

Fig. 2 shows this, together with the requirement in the CSR. It can be understood that the CSR requirement shown by the thin broken line is a considerable larger factor than Eq. (4).

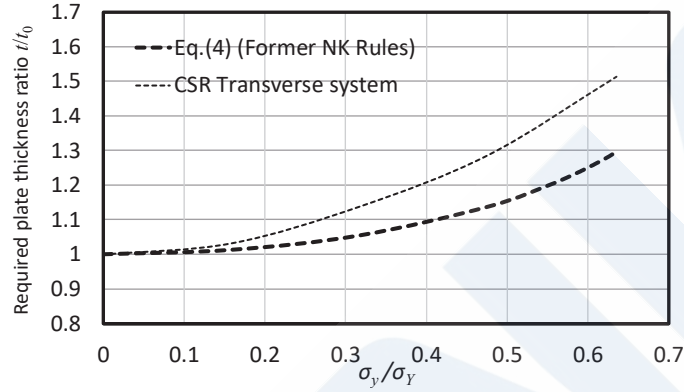


Fig. 2 Required plate thickness ratio depending on in-plane stress (transversely framed structure)

### 2.1.2 Longitudinally Framed Structures

In longitudinally framed structures, in-plane stress acts in the direction parallel to the stiffeners in Fig. 1, and in-plane stress and bending stress are orthogonal. In the former ClassNK Rules, the influence factor was formulated according to Tresca's yield criterion. Here, however, same as the transversely framed structure, an influence factor was newly derived using the von Mises yield criterion.

Assuming  $\sigma_{yu}$  is the bending stress of the plate upper surface,  $\sigma_{yl}$  is the bending stress of the plate lower surface, and  $\sigma_x$  is the in-plane stress acting in the  $x$  direction, the von Mises yield criteria for the plate upper and lower surfaces are given by the following Eqs. (5) and (6), respectively.

$$\sigma_{yu}^2 - \sigma_{yu}(\sigma_x + \nu_p \sigma_{yu}) + (\sigma_x + \nu_p \sigma_{yu})^2 = \sigma_Y^2 \quad (5)$$

$$\sigma_{yl}^2 - \sigma_{yl}(\sigma_x + \nu_p \sigma_{yl}) + (\sigma_x + \nu_p \sigma_{yl})^2 = \sigma_Y^2 \quad (6)$$

Next, if  $\eta$  is the range of  $\sigma_{yu}$  when a plastic hinge forms for the given plate thickness, the condition at which the axial load in the  $y$  direction becomes 0 is given as follows:

$$\sigma_{yu} \cdot \eta t + \sigma_{yl} \cdot (1 - \eta)t = 0 \quad (7)$$

$$\therefore \sigma_{yu} = -\frac{1 - \eta}{\eta} \sigma_{yl} \quad (8)$$

Substituting Eq. (8) into Eq. (5), and arranging the equation using  $\nu_p = 0.5$ ,

$$\frac{3}{4} \left( \frac{1 - \eta}{\eta} \right)^2 \sigma_{yl}^2 + \sigma_x^2 = \sigma_Y^2 \quad (9)$$

On the other hand, Eq. (6) can be transformed to,

$$\frac{3}{4}\sigma_{yl}^2 + \sigma_x^2 = \sigma_Y^2 \quad (10)$$

To satisfy Eq. (9) and Eq. (10) simultaneously, it can be understood that  $\eta = 1/2$ , and from Eq. (8),  $\sigma_{yu} = -\sigma_{yl}$ . Let's consider the meaning of this on the von Mises yield criterion curve in Fig. 3. If bending is applied gradually from a condition (point A) in which only an axial stress  $\sigma_x (>0)$  acts, the lower surface will yield first (point B), but the Poisson's ratio changes to 0.5 due to plasticizing before full section yielding is achieved, and  $\sigma_{yu} = -\sigma_{yl}$  irrespective of the value of  $\sigma_x$ . However, this is the case where  $\sigma_x$  is maintained. In reality, if bending is applied up to full section yielding,  $\sigma_x$  will be released from this position, the one-dot chain line will shift to the left, and the absolute values of  $\sigma_{yu}$  and  $\sigma_{yl}$  can increase to  $\alpha\sigma_Y$ .

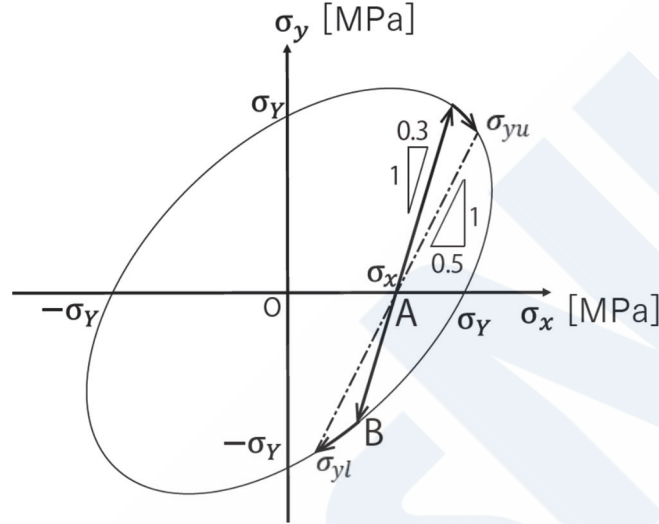


Fig. 3 Von Mises yield curve for plate bending in longitudinally framed structure

The following solution is obtained when Eqs. (9) and (10) are solved for  $\sigma_{yl}$ .

$$\sigma_{yl} = \frac{2\sqrt{3}}{3}\sqrt{\sigma_Y^2 - \sigma_x^2} = \alpha\sqrt{\sigma_Y^2 - \sigma_x^2} \quad (11)$$

Therefore, the fully plastic moment  $M_p$  is given by Eq. (12).

$$\begin{aligned} M_P &= \sigma_{yl} \cdot \frac{t}{2} \cdot \frac{t}{2} = \frac{\alpha\sigma_Y t^2}{4} \sqrt{1 - \left(\frac{\sigma_x}{\sigma_Y}\right)^2} = M_{P0} \sqrt{1 - \left(\frac{\sigma_x}{\sigma_Y}\right)^2} \\ \therefore \frac{M_P}{M_{P0}} &= \sqrt{1 - \left(\frac{\sigma_x}{\sigma_Y}\right)^2} \end{aligned} \quad (12)$$

Because the required plate thickness  $t$  is inversely proportional to the square root of Eq. (12), the ratio of  $t$  and the required thickness  $t_0$  when an axial load does not act on the member is as follows:

$$\frac{t}{t_0} = \frac{1}{\left\{1 - \left(\frac{\sigma_x}{\sigma_Y}\right)^2\right\}^{\frac{1}{4}}} \quad (13)$$

Fig. 4 shows the required plate thickness ratio according to Eq. (13) (red solid line) in comparison with the ratios in the former ClassNK Rules (black bold broken line) and CSR (black thin broken line). The in-plane stress influence factor given by the

ClassNK equation based on Tresca's yield criterion shows there is no influence of in-plane stress until the in-plane stress reaches  $0.5 \sigma_y$ , and the influence rises sharply after exceeding that value. Likewise, the influence of in-plane stress in the CSR is also zero until in-plane stress reaches  $0.2 \sigma_y$ , but then takes a value close to that given by the above Eq. (13), even though the formulation is different.

Table 1 summarizes the influence of in-plane stress on the fully plastic moment obtained by the von Mises yield criterion and the plate thickness ratios based on it.

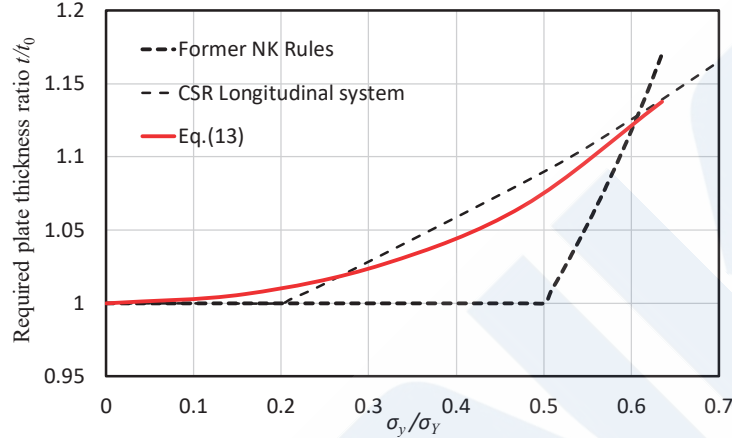


Fig. 4 Required plate thickness ratio by in-plane stress (longitudinally framed structure)

Table 1 Influence of in-plane stress on fully plastic moment

	Strength ratio	Required thickness ratio (Inverse square root of strength ratio)
Transversely framed structure (In-plane stress perpendicular to the longer edge)	$\frac{M_P}{M_{P0}} = 1 - \left(\frac{\sigma_y}{\sigma_Y}\right)^2$	$\frac{t}{t_0} = \frac{1}{\sqrt{1 - \left(\frac{\sigma_y}{\sigma_Y}\right)^2}}$
Longitudinally framed structure (In-plane stress parallel to the longer edge)	$\frac{M_P}{M_{P0}} = \sqrt{1 - \left(\frac{\sigma_x}{\sigma_Y}\right)^2}$	$\frac{t}{t_0} = \frac{1}{\left\{1 - \left(\frac{\sigma_x}{\sigma_Y}\right)^2\right\}^{1/4}}$

## 2.2 Influence of Additional Lateral Loading Accompanying In-Plane Stress

### 2.2.1 Formulation Considering Additional Lateral Loading

In transversely framed structures, the influence of additional lateral loading generated by in-plane stress is remarkable. To formulate this influence, a both-end fixed beam on which a tensile axial load  $N$  and a uniformly-distributed load  $w$  act, as shown in Fig. 5, will be considered. At this time, the equation related to deflection  $v$  considers the term  $N d^2v/dx^2$  for additional lateral loading term associated with the axial load, and is as follows, where  $E$  is young's modulus and  $I$  is the moment of inertia of area.

$$EI \frac{d^4v}{dx^4} = w + N \frac{d^2v}{dx^2} \quad (14)$$

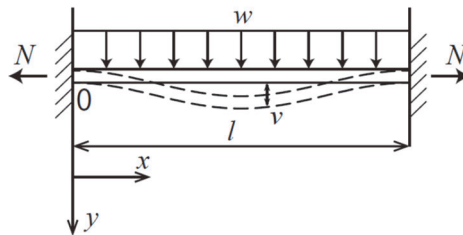


Fig. 5 Bending of plate under tensile axial load

If this equation is solved for the appropriate boundary condition, the load  $w_{2H-t}$  necessary for the formation of a 2-point plastic hinge and the deflection  $v_{2H-t}$  at that time, and the load  $w_{C-t}$  necessary for the formation of a 3-point plastic hinge and the accompanying deflection  $v_{C-t}$  is obtained as follows:

$$w_{2H-t} = \frac{2NM_P(e^{\beta l} - 1)}{EI(\beta l + \beta l e^{\beta l} - 2e^{\beta l} + 2)} \quad (15)$$

$$v_{2H-t} = \frac{w_{2H-t}l(1 - e^{\frac{\beta l}{2}})}{2\beta N(1 + e^{\frac{\beta l}{2}})} + \frac{w_{2H-t}l^2}{8N} \quad (16)$$

$$w_{C-t} = \frac{NM_P}{EI} \left( \frac{1 + e^{\frac{\beta l}{2}}}{1 - e^{\frac{\beta l}{2}}} \right)^2 \quad (17)$$

$$v_{C-t} = -\frac{\frac{M_P}{EI} + \frac{w_{C-t}}{N}}{\beta^2(1 + e^{\beta l})} \left( e^{\frac{\beta l}{2}} - 1 \right)^2 + \frac{w_{C-t}l^2}{8N} \quad (18)$$

where,  $\beta = \sqrt{\frac{N}{EI}}$

When a compressive axial load acts, solution of an equation in which the signs of the term  $N d^2v/dx^2$  in Eq. (14) are reversed, where compression is taken as positive, gives the load  $w_{2H-c}$  necessary for the formation of a 2-point plastic hinge and the deflection  $v_{2H-c}$  at that time, and the load  $w_{C-c}$  necessary for the formation of a 3-point plastic hinge and the deflection  $v_{C-c}$  at that time, as follows.

$$w_{2H-c} = \frac{2NM_P(-1 + \cos\beta l)}{EI(\beta l \cdot \sin\beta l - 2 + 2\cos\beta l)} \quad (19)$$

$$v_{2H-c} = \frac{w_{2H-c}l \cdot \sin\frac{\beta l}{2}}{2\beta N(1 + \cos\frac{\beta l}{2})} - \frac{w_{2H-c}l^2}{8N} \quad (20)$$

$$w_{C-c} = \frac{NM_P}{EI} \frac{1 + \cos\frac{\beta l}{2}}{1 - \cos\frac{\beta l}{2}} \quad (21)$$

$$v_{C-c} = \frac{1}{\beta^2} \left( \frac{w_{C-c}}{N} - \frac{M_P}{EI} \right) \frac{1 - \cos\frac{\beta l}{2}}{\cos\frac{\beta l}{2}} - \frac{w_{C-c}l^2}{8N} \quad (22)$$

It may be noted that the Euler buckling load when the member is regarded as a both-end simply supported beam is  $N_E = \pi^2 EI/l^2$ , and the corresponding  $\beta$  is  $\beta = \pi/l$ . From Eq. (22), it can be understood that deflection diverges at this time.

### 2.2.2 Parametric Study of Influence of In-Plane Stress on Plate Bending Strength

The ratios of strength (ratio of the 2-point and 3-point plastic hinge formation loads) with and without the action of in-plane stress were obtained using Eqs. (15), (17), (19) and (21). Figs. 6 and 7 show the results for tensile in-plane stress, and Figs. 8 and 9 show the results for compressive in-plane stress. In these calculations,  $l = 800$  mm,  $E = 206\,000$  MPa and  $\sigma_Y = 315$  MPa. The black broken lines show the strength decrease when the influence of the additional lateral loading accompanying in-plane stress is not considered, in other words, the strength decrease according to Eq. (3).

From Figs. 6 and 7, under the action of tensile in-plane stress, it can be understood that the strength increases due to the effect of additional lateral loading, and that effect becomes more remarkable as the plate thickness becomes thinner. Moreover, that effect is also larger in 3-point plastic hinge formation than in 2-point plastic hinge formation. Regarding the 3-point plastic hinge load, almost no strength decrease can be seen up to approximately  $0.5 \sigma_Y$  when the plate thickness is 25 to 30 mm and up to about  $0.8 \sigma_Y$  when the plate thickness is 15 mm.

From Figs. 8 and 9, under the action of compressive in-plane stress, strength decreases due to the influence of additional lateral loading, and that effect becomes more pronounced as the plate thickness decreases. In the case of the 2-point plastic hinge formation load, strength decreases almost linearly with respect to in-plane stress (red solid line) when the plate thickness is approximately 20 mm. Similarly, for the 3-point plastic hinge formation load, a nearly linear decrease in strength against in-plane stress (red solid line) is observed when the plate thickness is approximately 25 mm. When the plate thickness is less than the above value, the strength is further reduced. However, because this thinner plate thickness is supposed to be increased substantially by the buckling criteria separately, the red lines can be considered to be the substantial lower limit of the strength decrease. Therefore, the required plate thickness equation, Eq. (23), which is based on the linear strength reduction shown by the red lines and  $(\text{strength ratio}) = 1 - \sigma_y / \sigma_Y$ , is one guideline for the in-plane stress influence factor in transversely framed structures in which compressive in-plane stress acts.

$$\frac{t}{t_0} = \frac{1}{\sqrt{1 - \frac{\sigma_y}{\sigma_Y}}} \quad (23)$$

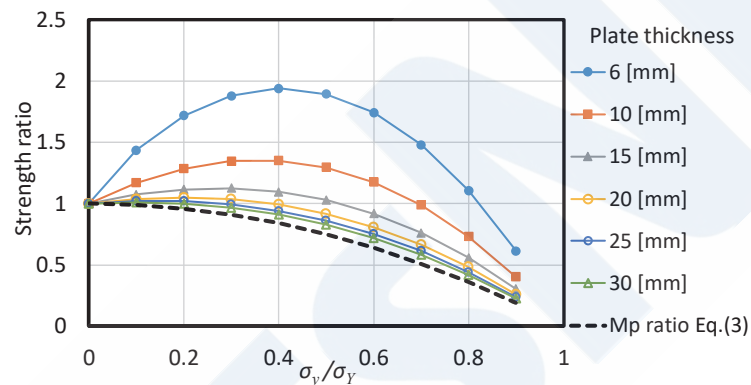


Fig. 6 2-point plastic hinge formation load ratio (tensile in-plane stress)

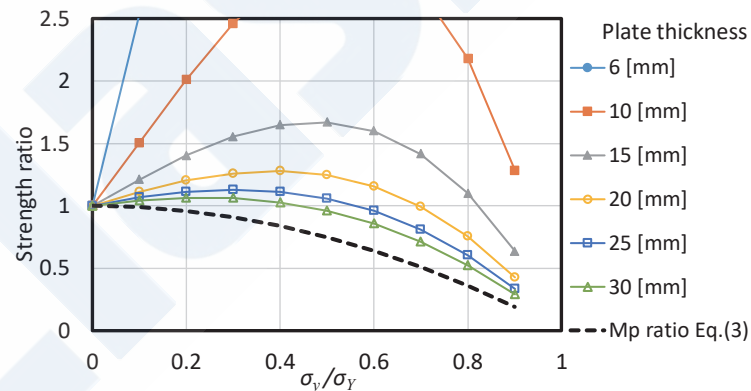


Fig. 7 3-point plastic hinge formation load ratio (tensile in-plane stress)

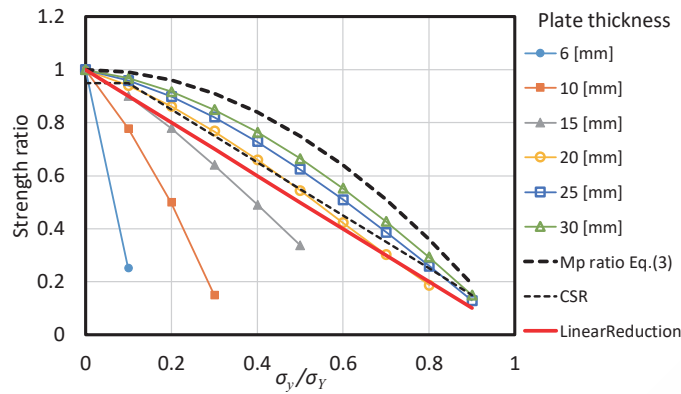


Fig. 8 2-point plastic hinge formation load ratio (compressive in-plane stress)

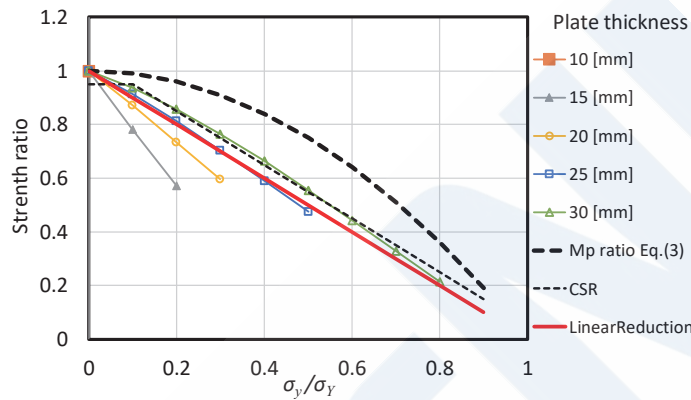


Fig. 9 3-point plastic hinge formation load ratio (compressive in-plane stress)

### 2.3 Verification of Theoretical Equations by Elasto-Plastic FEM

In this section, the theoretical equations derived up to the previous section will be verified by elasto-plastic FEM. Fig. 10 shows the FEM model. To eliminate the influence of the aspect ratio in accordance with the formulation up to the previous section, a sufficiently long panel with dimensions of 800 mm x 8 000 mm was assumed, and a 2 longitudinal space x 2 transverse space member was modeled. At the center of the long side (point A), the mesh was subdivided so that the element side length was 2.5 mm in order to detect the stress and bending moment. In addition, the displacement is detected at the center of the panel (point B). The analysis was conducted by the implicit method of LS-DYNA using Belytschko-Tsay shell elements with 6 integration points in the plate thickness direction, assuming Young’s modulus = 206 000 MPa, Poisson’s ratio = 0.3, tangent modulus = 0 and yield stress = 315 MPa. To model an infinitely continuing stiffened plate, a periodic boundary condition was adopted all around the model. As the loading procedure, after first applying various in-plane loads, lateral pressure loading was applied by incremental loading to the specified lateral pressure, after which both the lateral pressure and the in-plane load were removed (unloaded), and the stresses, bending moments and deflections at points A and B in this process and the residual deflection after unloading were observed.

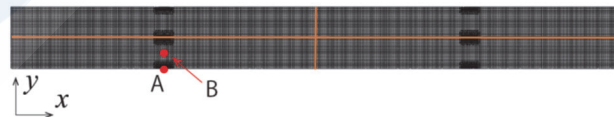
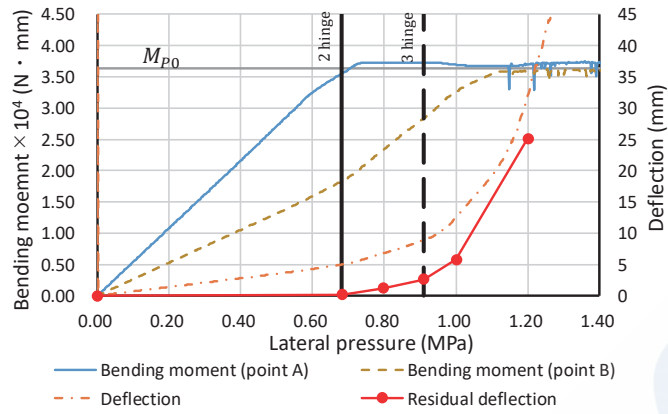


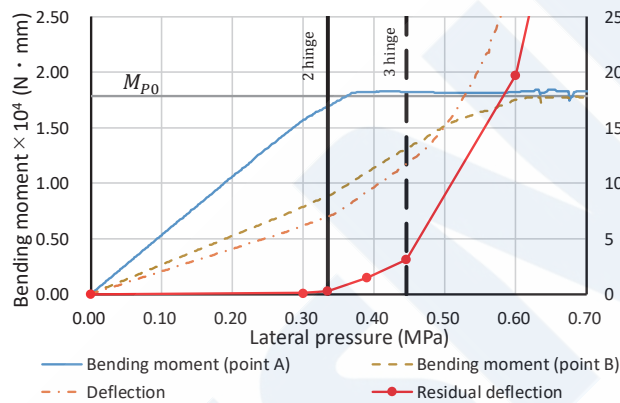
Fig. 10 Analysis model

#### 2.3.1 Case without In-Plane Stress

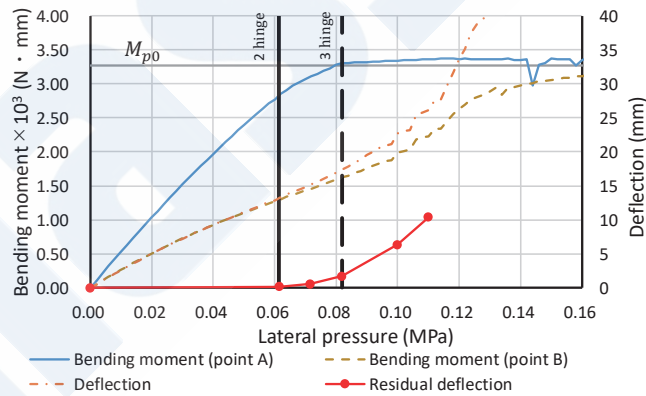
Fig. 11 shows the transition of the bending moment, deflection and residual deflection at points A and B with respect to the increment of lateral pressure for the plate thicknesses of 20 mm, 14 mm and 6 mm. In this figure, the vertical solid lines and vertical broken lines represent the 2-point plastic hinge formation load and the 3-point plastic hinge formation load, respectively.



(1) Plate thickness: 20 mm



(2) Plate thickness: 14 mm



(3) Plate thickness: 6 mm

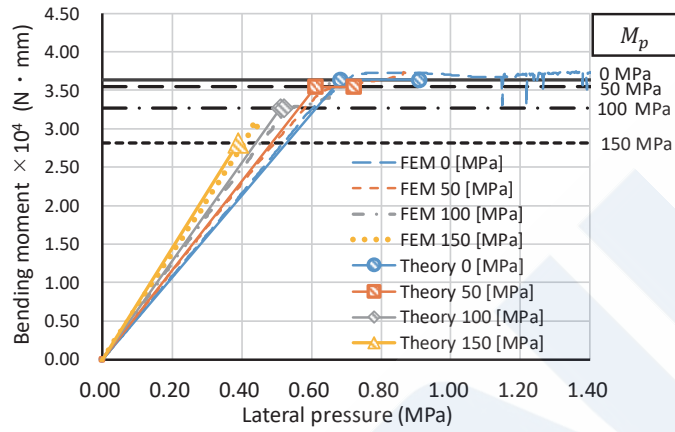
Fig. 11 Transitions of bending moment and deflection by lateral pressure

The bending moment at the center of the long side (point A) reaches a plateau at the fully plastic moment  $M_{p0}$ , and the lateral pressure at this time is roughly in agreement with the calculated 2-point plastic hinge formation load, excluding the case of the 6 mm plate thickness. On the other hand, although the bending moment in the panel center (point B) also reaches a plateau at  $M_{p0}$ , a substantially larger load than the 3-point plastic hinge formation load is required in order to reach  $M_{p0}$ . This tendency is particularly remarkable when the plate thickness is thin, and furthermore, when the plate thickness is 6 mm, a slight delay in 2-point plastic hinge formation is observed. These tendencies are the result of membrane stress supporting the lateral load. Although the effect is slight until formation of a 2-point plastic hinge, these effects cannot be ignored in 3-point plastic hinge formation. When residual deflection is observed, large growth of residual deflection begins regardless of the plate thickness if the applied load is larger than the 2-point plastic hinge formation load. Based on these facts, it appears to be appropriate to use

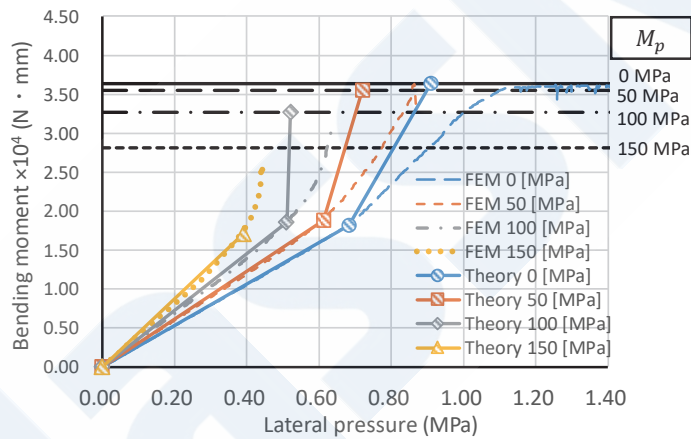
2-point plastic hinge formation as a criterion for establishing strength standards based on residual deflection criteria, as described in the following.

### 2.3.2 Case Where In-Plane Stress Acts on Transversely Framed Structure

Figs. 12 and 13 show the bending moment at the center of the long side (point A) and the center of the panel (point B) for the cases where compressive in-plane stress and tensile in-plane stress act on a structure, respectively. Here, the plate thickness is 20 mm.

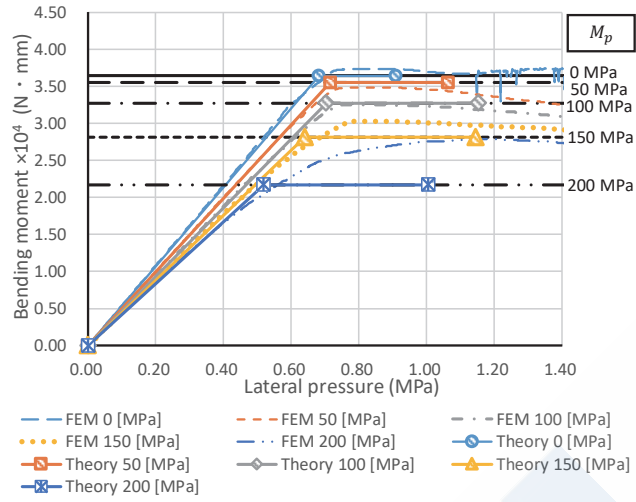


(1) Center of long side (point A)

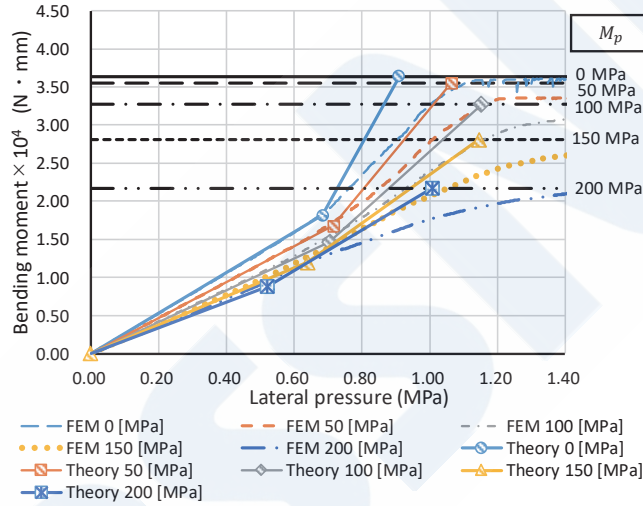


(2) Center of panel (point B)

Fig. 12 Transition of bending moment when compressive in-plane stress acts on a transversely framed structure



(1) Center of long side (point A)



(2) Center of panel (point B)

Fig. 13 Transition of bending moment when tensile in-plane stress acts on a transversely framed structure

In these figures, the broken lines and one-dot chain lines show the FEM results, and the solid lines show the theoretical calculations derived in the previous section. The several black horizontal lines in the figures are the fully plastic moment corresponding to the respective in-plane stresses obtained by Eq. (3). The markers attached to the theoretical calculation results are the positions of 2-point plastic hinge and 3-point plastic hinge formation given by Eqs. (15), (17), (19) and (21), respectively. Comparing the FEM and theoretical equation results, the two are in good agreement until formation of the 2-point plastic hinge, but after that point, the results diverge due to the effect of membrane stress. When compressive in-plane stress acts, the slope of the graphs becomes larger due to the effect of the additional lateral loading associated with the increase in in-plane stress. Together with the decrease in the fully plastic moment  $M_p$  accompanying in-plane stress, this greatly reduces the 2- and 3-point plastic hinge formation loads. Conversely, when tensile in-plane stress acts, the slope of the graphs decreases as the in-plane stress increases. In this case, with the balance of the strength increase due to the decrease in the slope and the strength decrease due to the decrease in  $M_p$ , a tendency in which strength increases once accompanying an increase in in-plane stress and then begins to decrease can also be observed from the graphs.

### 2.3.3 Case Where In-Plane Stress Acts on Longitudinally Framed Structure

Next, Fig. 14 shows the transition of the bending moment at the center of the long side (point A) when compressive in-plane stress acts on a longitudinally framed structure. The several black horizontal lines in the figure are the fully plastic moment corresponding to the in-plane stresses obtained by Eq. (12) for a longitudinally framed structure. Because the effect of in-plane stress on the fully plastic moment is small compared with that in a transversely framed structure, the amount of decrease in the

fully plastic moment due to in-plane stress is small in comparison with Fig. 12 and Fig. 13, which were based on Eq. (3). Since additional lateral loading due to in-plane stress does not act on a longitudinally framed structure, the slopes of the various lines are substantially identical regardless of the magnitude of the in-plane stress. Although the figure for the panel center (point B) is omitted here, almost no difference due to the action of in-plane stress was observed at the panel center and under the action of tensile in-plane stress.

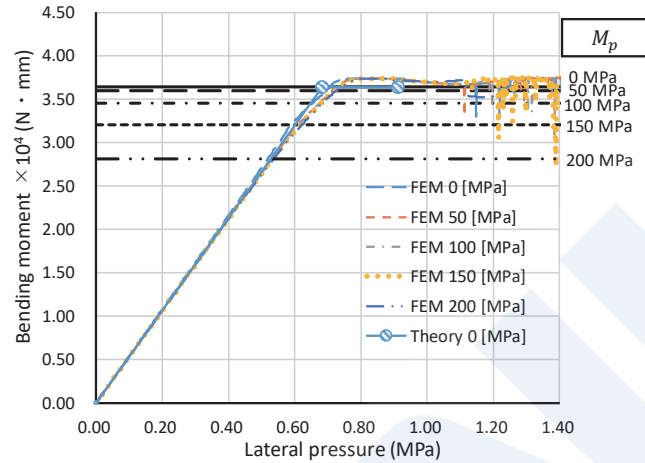


Fig. 14 Transition of bending moment at center of long side (point A) when compressive in-plane stress acts on a longitudinally framed structure

It is conceivable that a plastic hinge forms at point A when the lines in Fig. 14 reach the horizontal line representing the fully plastic moment corresponding to each in-plane stress. However, even under the action of in-plane stress, it can be seen that the bending moment calculated by FEM passes through the corresponding theoretical fully plastic moment and becomes a plateau on reaching the value  $M_{P0}$ , that is, the fully plastic moment without in-plane stress. This suggests the possibility that the fully plastic moment can substantially be supported in this cross section in case in-plane stress does not act, and the effect of in-plane stress on strength is extremely small in a longitudinally framed structure. In order to examine the reason for this, Fig. 15 shows the stress history of the upper surface and lower surface at point A when lateral pressure was gradually applied to a panel under the action of tensile in-plane stress of 200 MPa. Here, light blue shows the stress in the  $x$  direction, orange shows the stress in the  $y$  direction, black represents the von Mises stress, and the solid lines and broken lines show the values for the top surface and the bottom surface, respectively.

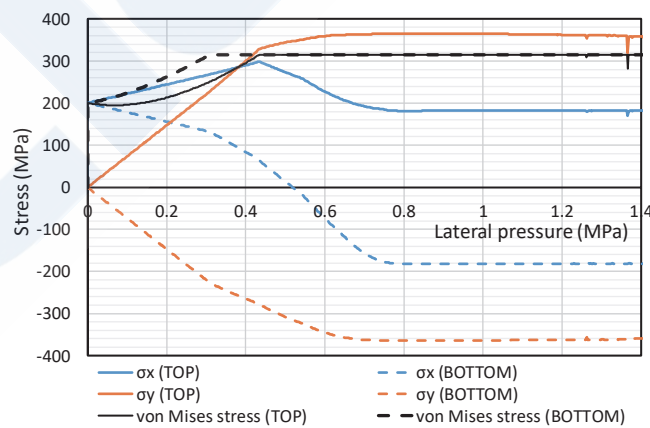


Fig. 15 Transition of surface stress condition at point A (longitudinally framed structure, tensile stress: 200 MPa)

When application of lateral pressure begins,  $y$ -direction bending stress is generated in opposite directions on the top and bottom surfaces, and the  $x$ -direction stress changes from the initial value of 200 MPa by an amount equivalent to the value obtained by multiplying that stress by the Poisson's ratio of 0.3. The slope of the bottom surface stress changes accompanying

yielding of the bottom surface at the lateral pressure of 0.31 MPa, and next, the top surface yields at the lateral pressure of 0.43 MPa, and the slope of the top surface stress also changes. When further lateral pressure is applied, the in-plane stress is released and the  $x$ -direction stress settles to  $\nu_p (= 0.5) \cdot \sigma_y$ , while  $\sigma_y$  continues to increase even after yielding and reaches  $\alpha (= 1.15) \cdot \sigma_Y$  when the lateral pressure is about 0.78 MPa. This condition is shown on the von Mises stress criterion curve in Fig. 16. That is, when further lateral pressure is applied after yielding of the bottom surface (●) and the top surface (■), it can be understood that the phenomenon observed in Fig. 3 where Poisson's ratio changes to 0.5 while maintaining the in-plane stress in the  $x$  direction does not occur, but instead the stress moves in the direction where the  $x$ -direction in-plane stress will be released.

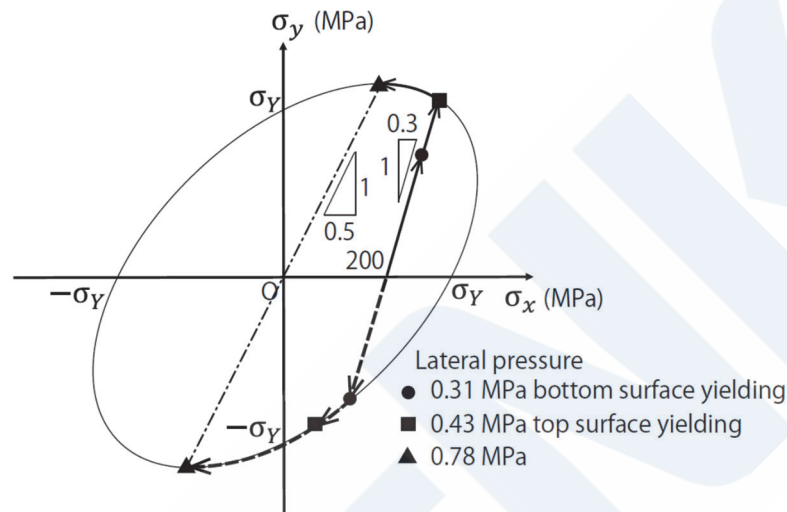


Fig. 16 Von Mises yield criterion curve for plate bending in a longitudinally framed structure (transition of stress in FEM results)

This fact means that the influence of in-plane stress on plate bending strength is eliminated if an extremely large lateral load is applied. However, at the timing of 2-point plastic hinge formation (calculated: 0.527 MPa), the  $x$ -direction in-plane stress still has not been released, and residual deflection begins to increase by the formation of the 2-point plastic hinge. Based on these facts, it is thought to be appropriate to consider the decrease in the fully plastic moment due to in-plane stress when placing the plate strength criterion on 2-point plastic hinge formation.

### 3. SERIES ANALYSIS OF ELASTO-PLASTIC FEM BASED ON RESIDUAL DEFLECTION CRITERION

As also pointed out by Hughes et al.<sup>10) 11)</sup>, because plate members which are subjected to lateral pressure have extremely large ultimate strength due to the effect of membrane stress, etc., an index based on the serviceability like residual deflection is useful as a design criterion. Therefore, in this chapter, series calculations by elasto-plastic FEM were carried out using residual deflection as a criterion, the effect of in-plane stress on plate bending strength was arranged, and a comparative study with the equations derived in Chapter 2 was conducted. The FEM model used here was the same as that used in Chapter 2, and we obtained the lateral pressure which causes the specified residual deflection by iterative FEM calculations at each level of in-plane stress. Since residual deflection began to increase when the load exceeded a load equivalent to 2-point plastic hinge formation regardless of the plate thickness, as in Chapter 2, it was considered appropriate to use 2-point plastic hinge formation as a strength criterion. Therefore, residual deflection of 0.26 mm which was generated when the 2-point plastic hinge formation load was applied to a 14-mm plate without in-plane stress was adopted as a common criterion.

#### 3.1 Results of Analysis of Transversely Framed Structure

Fig. 17 shows the relationship between the plate thickness and lateral pressure when residual deflection is 0.26 mm for the case where compressive in-plane stress acts on a transversely framed structure. When in-plane stress increases, the lateral pressure decreases remarkably at the same plate thickness, and conversely, the plate thickness for the same lateral pressure increases remarkably. Fig. 18 shows the result of plotting the strength ratio with respect to the case without in-plane stress,

where in-plane stress is shown on the horizontal axis. The FEM results show a tendency which is consistent with the graph of the strength ratio for the 2-point plastic hinge formation load shown in Fig. 8. The linear strength decrease equation (shown by the red solid line) covers the FEM results on the safe side. For reference, if the same calculation is performed with residual deflection set to 4 mm, the effect of in-plane stress becomes more pronounced, and the results approach the graph of the theoretical values of the strength ratio for the 3-point plastic hinge formation load shown in Fig. 9. Fig. 19 shows the relationship between compressive in-plane stress and the required plate thickness ratio. The required plate thickness ratio in the FEM result is larger than that by Eq. (4) in the former ClassNK Rules, and deviates both above and below the required values in the CSR. Although the required plate thickness ratio when lateral pressure is small (i.e., when the plate thickness is small) is larger than the CSR requirement, the linear strength decrease equation (Eq. (23); red solid line) covers the FEM results on the safe side.

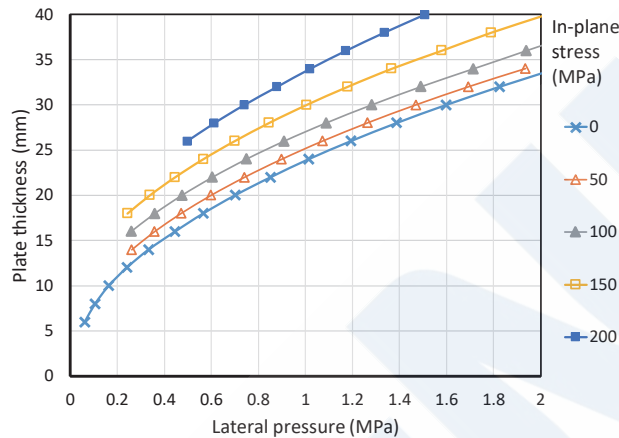


Fig. 17 Relationship between plate thickness and lateral pressure (transversely framed structure, compressive in-plane stress)

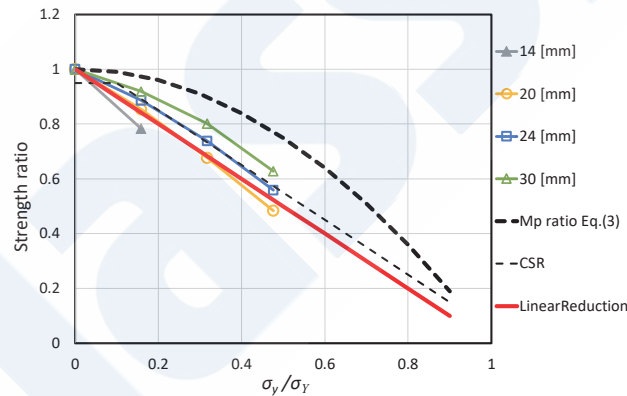


Fig. 18 Relationship between compressive in-plane stress and strength ratio (transversely framed structure)

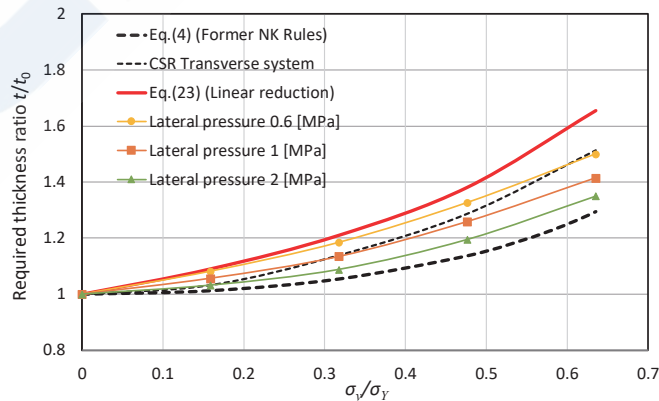


Fig. 19 Relationship between compressive in-plane stress and required plate thickness ratio (transversely framed structure)

Next, Fig. 20, Fig. 21 and Fig. 22 show similar figures for the case where the in-plane stress is tensile stress. Fig. 20 shows that the variation of each line due to the difference in the in-plane stress is smaller than that in Fig. 17, indicating that the influence of tensile in-plane stress on strength is small. In particular, when lateral pressure is small, in other words, when the plate thickness is small, a range where strength increases due to the action of tensile in-plane stress is observed. Here, it was found that Fig. 21, which shows the strength ratio for cases without the action of in-plane stress, displays a tendency which is in agreement with the graph of the theoretical values of the strength ratio for the 2-point plastic hinge formation load under the action of tensile in-plane stress in Fig. 6. In this case, the fully plastic moment ratio (Eq. (3), bold black broken line) based on the von Mises yield criterion adopted in the former ClassNK Rules covers the FEM results on the safe side. It should be noted that the influence of in-plane stress becomes more remarkable when the same calculation is performed with the residual deflection set to 4 mm for reference, and the result approached the graph of the theoretical values of the strength ratio for the 3-point plastic hinge formation load in Fig. 7. In the relationship between tensile in-plane stress and the required plate thickness in Fig. 22, the required plate thickness ratio in the FEM results falls even further below that of the former ClassNK Rules (Eq. (4), bold black broken line), which has the smallest required plate thickness ratio, and this covers the FEM results on the safe side. The strength increases due to tensile in-plane stress when lateral pressure is small (i.e., when the plate thickness is small), and the required plate thickness ratio falls below 1.0. This tendency becomes more remarkable in the calculation when the residual deflection criterion is set to 4 mm, and a strength decrease is not observed in almost all cases. However, with the criterion of 0.26 mm, which is equivalent to 2-point plastic hinge formation, that is, the point where growth of residual deflection begins, a clear effect on in-plane stress is observed, as can be seen in Fig. 22. Therefore, the design will be on the dangerous side if this effect is ignored.

To summarize the influence of compressive and tensile in-plane stress on transversely framed structures, the required plate thickness ratio given by the FEM results is covered on the conservative side by Eq. (23) using the linear strength decrease in the case of compressive in-plane stress, and by Eq. (4), which is based on the von Mises yield criterion, in the case of tensile in-plane stress. In this case, the safety margin for compression increases when the plate thickness is large, while the safety margin for tension increases when the plate thickness is small.

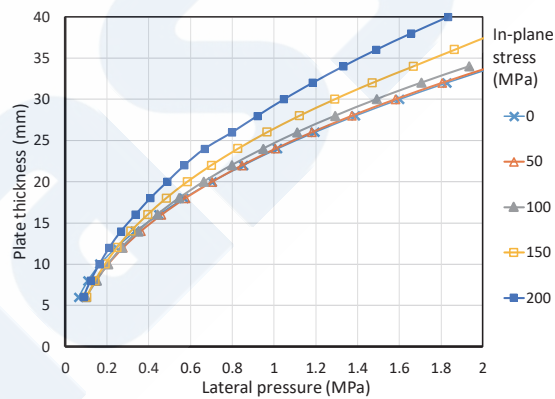


Fig. 20 Relationship of plate thickness and lateral pressure (transversely framed structure, tensile in-plane stress)

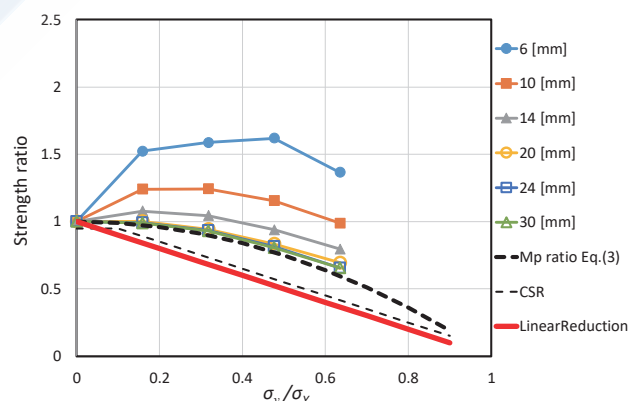


Fig. 21 Relationship of tensile in-plane stress and strength ratio (transversely framed structure)

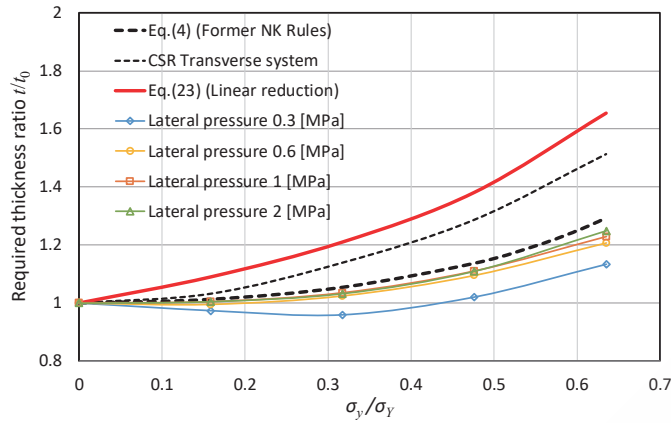


Fig. 22 Relationship of tensile in-plane stress and required plate thickness ratio (transversely framed structure)

### 3.2 Results of Analysis for Longitudinally Framed Structures

Similar figures for the case where compressive in-plane stress acts on a longitudinally framed structure are shown in Fig. 23, Fig. 24 and Fig. 25. As can be seen in Fig. 23, the influence of in-plane stress is quite small, but occurs in the same manner regardless of the level of lateral pressure. As shown in the strength ratio in Fig. 24, the influence of in-plane stress is disregarded up to  $0.5\sigma_Y$  in the former ClassNK Rules and up to  $0.2\sigma_Y$  in the CSR. However, the FEM results show a slight decreasing tendency from the stage where in-plane stress is small, and Eq. (12) (red solid line), which is based on the von Mises yield criterion, expresses that tendency well on the safe side. Likewise, in Fig. 25, which is arranged by the required plate thickness, Eq. (13) (red solid line) based on the von Mises yield criterion also covers the FEM results on the safe side.

The case of tensile in-plane stress gave results that were substantially the same as the case of compression. Moreover, if summarized using the 4 mm residual deflection criterion, the influence of in-plane stress is small to a level that is almost negligible. This is considered to be the result of a phenomenon in which in-plane stress is released from the plastic hinge formation site, as explained in Section 2.3.3.

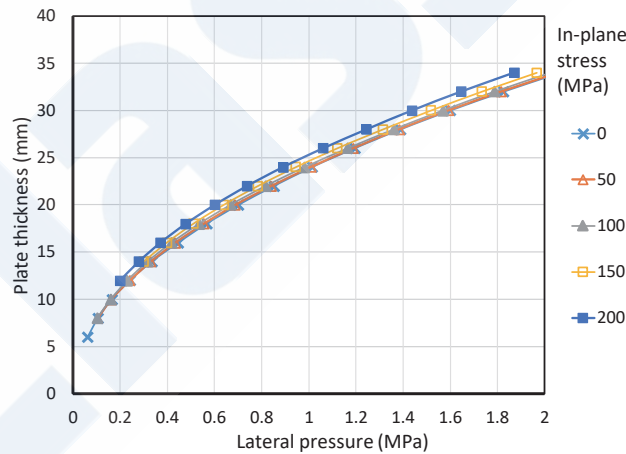


Fig. 23 Relationship of plate thickness and lateral pressure (longitudinally framed structure, compressive in-plane stress)

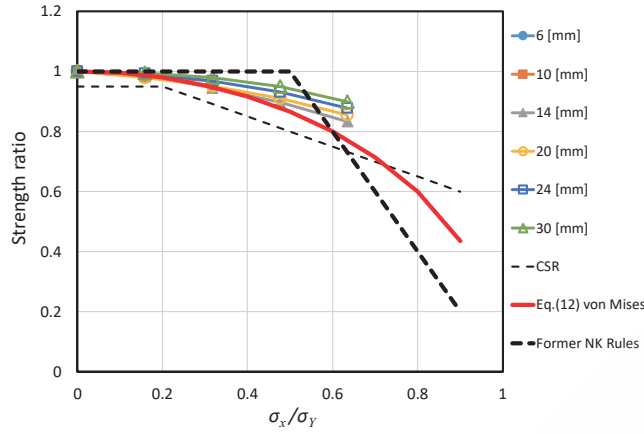


Fig. 24 Relationship of compressive in-plane stress and strength ratio (longitudinally framed structure)

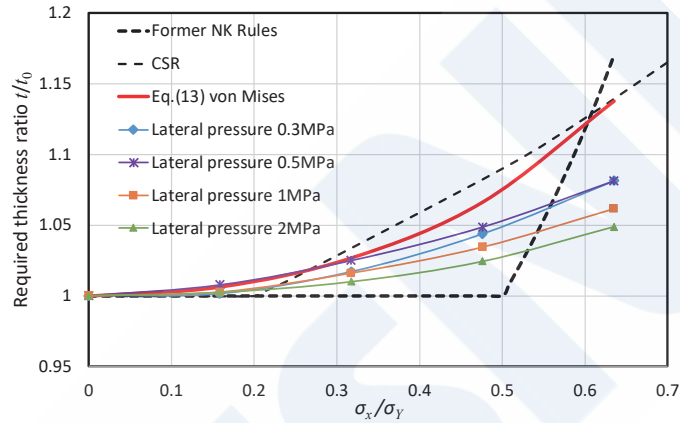


Fig. 25 Relationship of compressive in-plane stress and required plate thickness ratio (longitudinally framed structure)

Table 2 In-plane stress influence factors (strength ratio) and required plate thickness ratio

		Applied criterion	In-plane stress influence factor $C_a$ (Strength ratio)	Required thickness ratio $t/t_0$
Longitudinally framed structure		Von Mises criterion with orthogonal in-plane and bending stress	$\sqrt{1 - \left(\frac{\sigma_x}{\sigma_Y}\right)^2}$ (12)	$1/\left(1 - \left(\frac{\sigma_x}{\sigma_Y}\right)^2\right)^{1/4}$ (13)
Trans-versely framed structure	Tension	Von Mises criterion with parallel in-plane and bending stress	$1 - \left(\frac{\sigma_y}{\sigma_Y}\right)^2$ (3)	$1/\sqrt{1 - \left(\frac{\sigma_y}{\sigma_Y}\right)^2}$ (4)
	Compression	Linear strength reduction	$1 - \frac{ \sigma_y }{\sigma_Y}$	$1/\sqrt{1 - \frac{ \sigma_y }{\sigma_Y}}$ (23)

### 3.3 Summary of In-Plane Stress Factors

Based on the results presented above, Table 2 summarizes the strength ratios and scantling formulae (required plate thickness ratios) which are capable of covering the FEM results on the safe side. These are the von Mises yield criterion (Eq. (13)) for cases where in-plane stress and bending stress act orthogonally for longitudinally framed structures, the von Mises yield criterion (Eq. (4)) for cases where in-plane stress and bending stress act in the same direction for transversely framed structures under tension, and the linear strength decrease criterion (Eq. (23)) for transversely framed structures under compression.

#### 4. COMBINED INFLUENCE OF IN-PLANE STRESS AND ASPECT RATIO

Up to the previous chapter, cases in which the aspect ratio of plate members was sufficiently large were examined, and it was shown that the influence of in-plane stress differs greatly in longitudinally framed structures and transversely framed structures. However, if the same in-plane stress influence factors are also applied to cases where the aspect ratio is small, the results will be irrational, since the required plate thickness becomes discontinuous depending on whether the aspect ratio is larger or smaller than 1.0. In reality, in such cases, it is thought that an intermediate in-plane stress influence between that of a longitudinally framed structure and a transversely framed structure acts on the member.

On the other hand, an aspect ratio correction factor is introduced in the scantling formulae in the CSR and other standards in order to consider the strength increase when the aspect ratio of a plate member is small, but this is treated independently from the in-plane stress factor. Therefore, this chapter will examine a method for rationally interpolating the in-plane stress influence factor between those of a longitudinally framed structure and a transversely framed structures, and a combined influence factor of this interpolated in-plane stress influence factor and the aspect ratio correction factor.

##### 4.1 Derivation of Combined Influence Factor

In cases where in-plane stress acts, strength decreases by the ratio  $C_a$  as shown in Table 2, depending on whether the structure is longitudinally framed or transversely framed and whether the in-plane stress is compressive or tensile. These  $C_a$  ratios can all be expressed by generalization to the form of Eq. (24). Therefore, the influence of in-plane stress for small aspect ratios is considered to be expressed rationally by appropriately correcting  $\alpha$  and  $\beta$  in Eq. (24) between the longitudinally framed structure and transversely framed structure.

$$C_a = \left\{ 1 - \left( \frac{|\sigma_{BM}|}{\sigma_Y} \right)^\alpha \right\}^\beta \quad (24)$$

Here,  $\sigma_{BM}$  is the hull girder vertical bending stress. In this chapter, only the hull girder vertical bending stress will be considered as the in-plane stress. Based on this assumption, when the aspect ratio is large, in a longitudinally framed structure,  $\alpha = 2$ ,  $\beta = 1/2$ , and in a transversely framed structure,  $\alpha = 2$ ,  $\beta = 1$  when the in-plane stress is tensile and  $\alpha = 1$ ,  $\beta = 1$  when the in-plane stress is compressive.

Next, regarding the aspect ratio correction factor, in the previous chapter, 2-point plastic hinge formation was adopted as the criterion for the in-plane stress influence factor. Therefore, here, the aspect ratio correction factor will be studied based on plate elastic bending theory. Using the series solutions<sup>12)</sup> of the bending moments at the center of the long side and center of the short side of a rectangular plate with a finite aspect ratio and four fixed sides subjected to a uniformly distributed load, an approximate expressions for the required plate thickness ratio to the required plate thickness  $t_\infty$  when the aspect ratio =  $\infty$  and the short side length is the same were obtained as shown in Eqs. (25) and (26).

$$C_{Aspect-L} = \min \left( 1.07 - 0.28 \left( \frac{\min(l, s)}{\max(l, s)} \right)^2, 1 \right) \quad (25)$$

$$C_{Aspect-S} = \min \left( 0.84 - 0.05 \left( \frac{\min(l, s)}{\max(l, s)} \right)^4, 0.828 \right) \quad (26)$$

Here,  $l$  and  $s$  are the side length in the ship longitudinal direction and transverse direction, and  $C_{Aspect-L}$  and  $C_{Aspect-S}$  are the required plate thickness ratio considering the influence of the aspect ratio at the center of the long side and the short side, respectively. Because  $C_{Aspect-L}$  is always larger than  $C_{Aspect-S}$  when in-plane stress does not act,  $C_{Aspect-L}$  is adopted as the basis for the aspect ratio correction factor.

Next, the influence of in-plane stress on this will be considered. In a longitudinally framed structure, the influence of the in-plane stress on the center of the short side is larger than the influence on the center of the long side, which means a plastic hinge forms first on the center of the short side when the in-plane stress is large. If the structure is longitudinally framed, the influence

of additional lateral loading accompanying in-plane stress is assumed to be small even if the aspect ratio is small. Then, we examine the strength decrease expressed by Eq. (12) at center of the long side, and the strength decrease expressed by Eq. (3) at the center of the short side. Fig. 26 shows the required plate thickness ratio to the required plate thickness  $t_{0\infty}$  when the aspect ratio =  $\infty$  and the in-plane load is zero for aspect ratios in the range of 0.5 to 1.0 in a longitudinally framed structure. The black lines and red lines show the required plate thickness ratio based on bending at the center of the long side and bending at the center of the short side, respectively. The broken lines indicate the required plate thickness ratio when in-plane stress is zero (i.e., the above-mentioned Eqs. (25) and (26)), and the solid lines are the required plate thickness ratio when the in-plane stress  $\sigma_{BM} = 0.5\sigma_Y$  acts.

As the aspect ratio approaches 1.0, the required plate thickness ratio with respect to  $t_{0\infty}$  decreases in accordance with Eq. (25), as shown by the black broken line, and plastic hinges form simultaneously at the centers of the long side and the short side at the aspect ratio of 1.0. On the other hand, if in-plane stress acts on the member, the influence on the center of the short side is larger, and as a result, in this case, a plastic hinge forms first at the center of the short side at about  $s/l > 0.83$ . Based on the above, we tried setting  $\alpha$  and  $\beta$  so that  $\alpha = 2$  and  $\beta = 1$  when the aspect ratio is 1.0. In this case, when the aspect ratio changes from 1.0 in a longitudinally framed structure, the result is an interpolation that takes the envelope of the two solid lines in Fig. 26 on the safe side. When the aspect ratio changes from 1.0 in a transversely framed structure and if the in-plane stress is compressive, the result is an interpolation in which the influence of additional lateral loading which is not considered when the aspect ratio is 1.0 appears progressively as the aspect ratio  $s/l$  becomes larger.

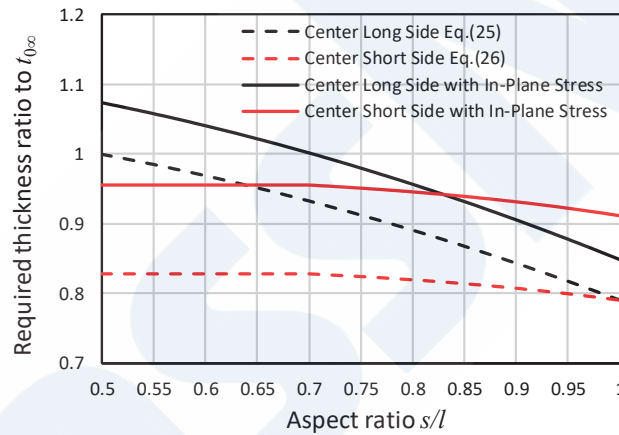


Fig. 26 Relationship of aspect ratio and required plate thickness ratio

Based on these points, when the influence of in-plane stress of a longitudinally framed structure is applied to aspect ratios of  $s/l < 0.5$  and the influence of in-plane stress of a transversely framed structure is applied to  $s/l > 2.0$ , and linear interpolations are performed between  $0.5 \leq s/l < 1.0$  and between  $1.0 \leq s/l \leq 2.0$ ,  $\alpha$  and  $\beta$  can be set as shown in Table 3.

Table 3 Interpolation of parameters  $\alpha$  and  $\beta$

	In-plane stress	$s/l$	$\alpha$	$\beta$
Longitudinally framed structure	Common to tensile and compressive	$\frac{s}{l} \leq 0.5$	2	0.5
		$0.5 \leq \frac{s}{l} \leq 1$	2	$\frac{s}{l}$
Transversely framed structure	Tensile	$1 \leq \frac{s}{l}$	2	1
	Compressive	$1 \leq \frac{s}{l} \leq 2$	$2\frac{l}{s}$	1
		$2 \leq \frac{s}{l}$	1	1

On this assumption, the combined influence factor of the in-plane stress influence factor and the aspect ratio correction factor can be expressed by the following equation:

$$\frac{t}{t_{0\infty}} = \frac{C_{Aspect-L}}{\sqrt{C_a}} = \frac{\min\left(1.07 - 0.28\left(\frac{\min(l,s)}{\max(l,s)}\right)^2, 1\right)}{\sqrt{\left\{1 - \left(\frac{|\sigma_{EM}|}{\sigma_Y}\right)^{\alpha\beta}\right\}}} \quad (27)$$

#### 4.2 Verification of Aspect Ratio Influence by Elasto-Plastic FEM

Here, as in Chapter 3, the plate thickness that gives residual deflection of 0.26 mm at each level of lateral pressure was obtained by repeated FEM calculations. The FEM model was the same as that used in Chapter 3, and the length of the short side was kept at 800 mm when changing the aspect ratio.

Fig. 27 shows the calculated results of the influence of the aspect ratio on the required plate thickness ratio when the in-plane stress is zero. The horizontal axis shows the aspect ratio  $s/l$  expressed on a logarithmic scale. The left half of the figure corresponds to a longitudinally framed structure, and the right half to a transversely framed structure. The black broken line and red solid line are the aspect ratio influence by Eq. (25) and the CSR method, respectively. The influence of the aspect ratio appears remarkably as the acting lateral pressure decreases, and Eq. (25), which is proposed in this paper, covers the FEM results on the safe side. Although the results by the correction equation according to the CSR also contain some points that are slight on the dangerous side, overall, those results are in good agreement with the FEM results.

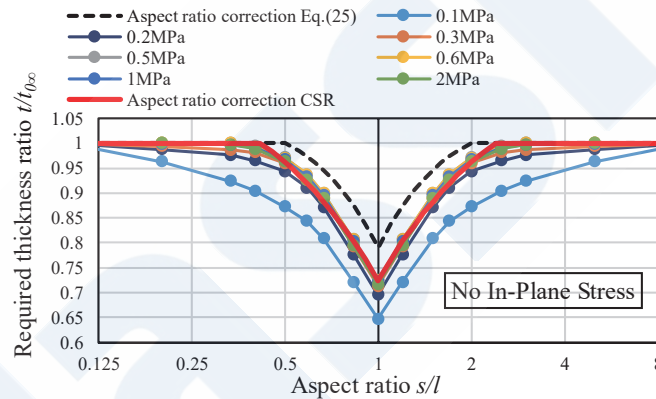


Fig. 27 Influence of aspect ratio without in-plane stress

Next, the calculated results of the aspect ratio influence with in-plane stress are shown in Fig. 28. The three figures on the left are cases of compressive in-plane stress, the three on the right are cases of tensile in-plane stress, where the magnitude of the in-plane stress, in order from the top, is  $0.3 \sigma_Y$ ,  $0.5 \sigma_Y$  and  $0.7 \sigma_Y$ . When the in-plane stress is compressive and the plate thickness is thin, there were cases where the calculation could not be continued due to buckling; those results are not included here (this occurred particularly in cases such as large in-plane stress in a transversely framed structure and a lateral pressure of 0.3 MPa or less, etc.). In addition, although calculation was possible, cases where the Euler buckling stress was less than the in-plane stress are indicated by the triangular markers ( $\blacktriangle$ ). In this figure, the black solid lines are the required plate thickness ratio according to Eq. (25), which does not consider the influence of in-plane stress, and the black broken lines are the required plate thickness ratio according to Eq. (27), which includes the influence of in-plane stress in this Eq. (25).

The black broken lines generally cover the FEM results to the safe side. In the case of compressive in-plane stress, the results partially exceed the black broken lines, but since these points are thought not to satisfy the Euler buckling stress (shown by the  $\blacktriangle$  marker), or to be close to that condition, it is thought that these should be covered by a separate buckling criterion. Between  $0.5 \leq s/l < 1.0$  in the longitudinally framed structure, a phenomenon in which the required plate thickness ratio increases once as the aspect ratio approaches 1.0 can be observed, particularly when the lateral pressure is small. Although the additional lateral loading associated with in-plane stress is disregarded in longitudinally framed structures, in actuality, some influence of

additional lateral loading occurs when the aspect ratio is near 1.0, and this is thought to be the cause of such behavior. Moreover, the fact that the graphs of the required plate thickness ratio shift to the opposite (lower) side at the corresponding locations when in-plane stress is tensile also support this conclusion. Based on the above, for tensile in-plane stress, a quite conservative assessment is obtained when the lateral pressure is small. Overall, however, the Eq. (27) proposed here gives a conservative assessment of the FEM results, and therefore can be considered a valid criterion.

## 5. CONCLUSION

This paper introduced the main content studied in connection with local strength formulae for plate members, which are the most basic element of ships, in the comprehensive revision of Part C of ClassNK's "Rules and Guidance for the Survey and Construction of Steel Ships." As a result, it is thought that the initial goal of revising these formulae as scantling formulae which are backed by theoretical equations and have a clearer correspondence with damage has been achieved to some extent.

While scantling formulae for plate members are fundamental, they are also affected in a complex manner by a variety of factors, and it is essential to develop formulae that are as simple as possible while quantitatively verifying the effects of the main factors. A more detailed analysis of cases where members are subjected to biaxial in-plane stress or shear stress, cases of initial irregularities such as plate distortion caused by welding, and the like, and study of how those problems can be covered by the equations in the Rules, are issues for the future.

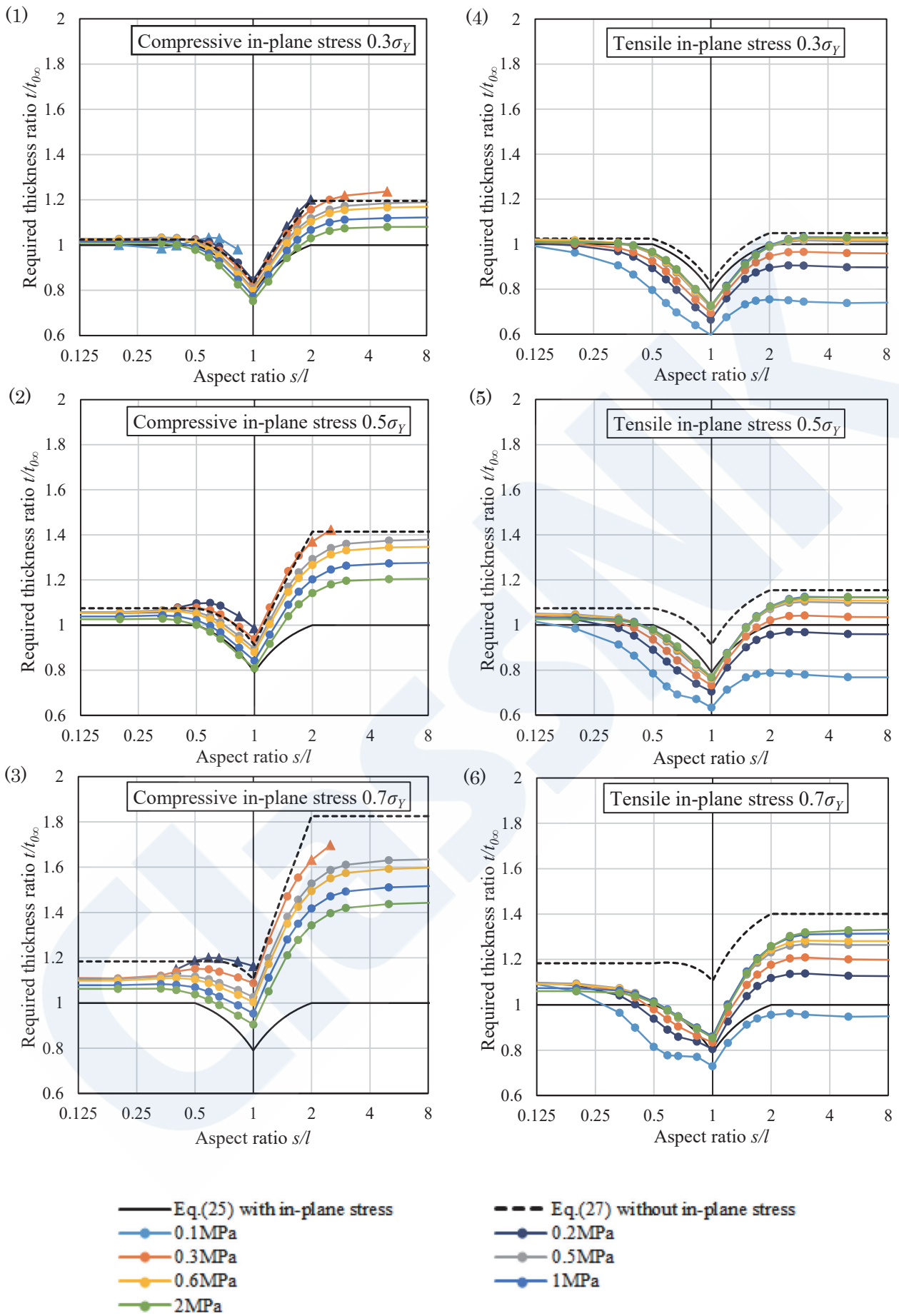


Fig. 28 Relationship of aspect ratio and required plate thickness ratio under action of in-plane stress

## REFERENCES

- 1) Okumoto, Y., Takeda, Y., Mano, M., Okada, T.: Part II, Chapter 5 Design of plates, in Design of ship hull structures – A practical guide for engineers, Springer, 2009
- 2) Yamamoto, Y.: Elasticity and Plasticity, Asakura Publishing Co., Ltd., 1961
- 3) Jones, N.: Plastic behavior of ship structures, Transactions of the Society of Naval Architects and Marine Engineers, pp.115-145, 1976
- 4) Nippon Kaiji Kyokai (ClassNK): 1980 Commentary on Revisions of Rules and Guidance for the Survey and Construction of Steel Ships, Transactions of Nippon Kaiji Kyokai No. 172, 1980
- 5) Nippon Kaiji Kyokai (ClassNK): 1961 Commentary on Revisions of Rules and Guidance for the Survey and Construction of Steel Ships, Transactions of Nippon Kaiji Kyokai No. 67, 1961
- 6) International Association of Classification Societies: Common structural rules for bulk carriers and oil tankers – technical background rule reference, 2020
- 7) Naruse, Y., Kim, M., Umezawa, R., Ishibashi, K., Koyama, H., Okada, T., Kawamura, Y.: Scantling evaluations of plates and stiffeners based on elasto-plastic analysis under axial loads and lateral pressures, In: Practical design of ships and other floating structures - proceedings of the 14th international symposium, PRADS2019, September 22-26, 2019, Volume II, Yokohama, Japan: Springer, pp. 100-127, 2021
- 8) Umezawa, R., Naruse, Y., Okada, T., Kawamura, Y., Ishibashi, K., Koyama, H.: A study on scantling formulae of plate members due to lateral pressure under the effect of axial loads, Marine Structures 80, 103099, 2021
- 9) Yamada, M., Okada, T., Naruse, Y., Kawamura, Y., Hayakawa, G., Ishibashi, K., Koyama, H.: Influence of plate aspect ratio on the axial load effect on the plate strength against lateral pressure, 15th International Symposium on Practical Design of Ships and Other Floating Structures, PRADS2022, Dubrovnik, Croatia, October 9<sup>th</sup> –13<sup>th</sup>, 2022
- 10) Hughes, O. F. et al.: Ship structural analysis and design, The Society of Naval Architects and Marine Engineers, 2010
- 11) Hughes, O. F.: Design of laterally loaded plating – uniform pressure loads, Journal of Ship Research, 25(2), pp.77-89, 1981
- 12) Timoshenko, S., Woinowsky-Krieger, S.: Theory of plates and shells, McGraw-Hill Book Company, New York, 2<sup>nd</sup> Edition, 1959